

A Model for the Estimation of Ankle and Hip Joints Visco-elastic Parameters During Balancing^{*}

Angel Cerda-Lugo^{*} Alejandro González^{**}
Antonio Cárdenas^{*} Davide Piovesan^{***}

^{*} Universidad Autónoma de San Luis Potosí

^{**} CONACyT-Universidad Autónoma de San Luis Potosí
Engineering Faculty; San Luis Potosí, San Luis Potosí, México;
(e-mail: angelcerda13@gmail.com).

^{***} Gannon University; Department of Mechanical Engineering; Erie,
PA, USA

Abstract: About 30% of the elderly population of the USA exhibits a motor impairment that inhibits daily activities and increases the probability of a fall. The ability of individuals to maintain proper balance is largely dependent on their control over their hip and ankle joints. Studying the mechanical behavior of these joints is important for the analysis of balancing compensatory motions. This paper presents a human balancing model based on a double inverted pendulum whose segments (representing the thorax and legs) are joined by a spring-damper system, creating a second order Kelvin-Voigt system. The model presented here allows for the estimation of constant apparent joint visco-elastic parameters when presented with a disturbance. The paper outlines the deduction of the model, shows initial results for the estimation of joint parameters using both simulated and experimental data.

Keywords: Visco-elastic parameters, Parameter estimation, Recursive estimation, Least squares, Dynamic model.

1. INTRODUCTION

Around 30% of the elderly population in the USA suffers from a form of motor impairment (Menz et al., 2005). This is known to have an influence in the high percentage of deaths this population experiences after suffering from a fall, especially when resulting in a broken leg or hip. Additionally, the low activity level which usually follows such events further negatively influences the health of the subject's cardio-respiratory system. This justifies the study of the human balance as a means of reducing fall risks. We seek to understand the stability margins of the human balancing system and how it is affected by the changes in the visco-elastic parameters of the joints. These parameters are task generally task dependent and obtaining their ranges could have clinical applications. For example, they could be used for early detection of fall risks or evaluating a subject's improvement after physical rehabilitation.

This article presents a second order dynamic model capable of describing human motion while balancing on the sagittal plane. The model we derive can be thought of as an

extension of the one presented by Chavez-Romero et al. (2014); it includes a hip joint and allows for the system's non-linearities. The dynamic model and parameter estimation are validated using simulations and experimental data. We then estimate the apparent joint stiffness and damping (Roberts and Azizi, 2011) using the *hold and release* paradigm proposed by Bortolami et al. (2003) while measuring only joint angles. Furthermore, the proposed dynamic model for parameters estimation can be applied in real-time.

2. A SECOND ORDER MODEL FOR BALANCING

It is possible to model the movement of the hip and ankle joints using a double inverted pendulum such as the one shown in Fig. 1-a). The pendulum's segments, representing the subject's legs and torso-head, are connected using a single degree-of-freedom joint and visco-elastic elements which act as the muscles and tendons (Piovesan et al., 2015). A second joint, with similar characteristics, connects the legs to the feet which are considered solidly attached to the ground. It is possible to estimate the apparent stiffness and damping at the joint by modeling the model's dynamics as described in Fig. 1-b).

^{*} Partially funded through the Catedras-CONACyT 972/2016 project

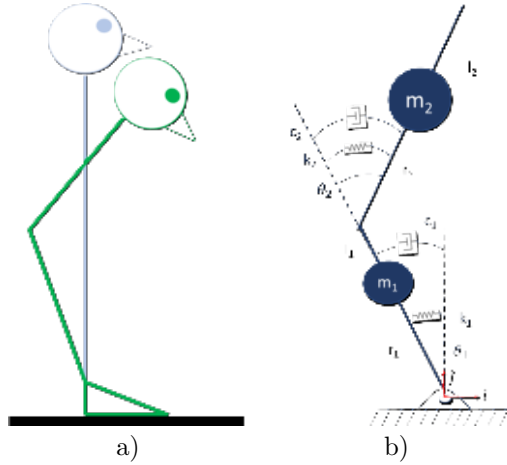


Fig. 1. A mechanical model representing balance using the hip strategy. a) Shows a sagittal plane view, while b) shows the double pendulum with visco-elastic parameters model developed.

The dynamic model can be obtained using the Euler-Lagrange formalism as follows (Meirovitch, 2010): Take the mass of the i -th segment is written as m_i , the distance between two consecutive joints l_i , the segment's center of mass position as measured from the distal joint as r_i gives, and the joint stiffness and damping represented by k_i and b_i respectively. Additionally, the generalized coordinates of the system are defined as $\mathbf{q} = [\theta_1 \ \theta_2]$. Using the unit vector $\hat{\mathbf{i}}$ running parallel to the ground plane and $\hat{\mathbf{j}}$ with a positive direction contrary to that of the action of gravity, the position of each mass (\mathbf{r}_{m_i}) is found to be:

$$\mathbf{r}_{m_1} = -r_1 \sin \theta_1 \hat{\mathbf{i}} + r_1 \cos \theta_1 \hat{\mathbf{j}} \quad (1)$$

$$\mathbf{r}_{m_2} = (-l_1 \sin \theta_1 + r_2 \sin \theta_{21}) \hat{\mathbf{i}} + (l_1 \cos \theta_1 + r_2 \cos \theta_{21}) \hat{\mathbf{j}} \quad (2)$$

where $\theta_{21} = \theta_2 - \theta_1$

The system's total kinetic energy is defined in terms of the segments' speed (\dot{r}_m) as:

$$T = \frac{1}{2} \left(m_2 \left(l_1^2 \dot{\theta}_1^2 + r_2^2 \dot{\theta}_{21}^2 - 2l_1 l_2 \dot{\theta}_1 \dot{\theta}_{21} \cos \theta_2 \right) + m_1 r_1^2 \dot{\theta}_1^2 + I_1 \dot{\theta}_2^2 + I_2 \dot{\theta}_{21}^2 \right) \quad (3)$$

where I_i is the moment of inertia of segment i .

The system's total potential energy, including that stored in the elastic elements, is given by:

$$V = m_1 g r_1 \cos \theta_1 + m_2 g (l_1 \cos \theta_1 + r_2 \cos \theta_{21}) + \frac{1}{2} (k_1 \theta_1^2 + k_2 \theta_2^2) \quad (4)$$

Finally, the energy dissipated by the dampers is (Ogata, 1998):

$$D = \frac{1}{2} (b_1 \dot{\theta}_1^2 + b_2 \dot{\theta}_2^2) \quad (5)$$

The Lagrangian is then defined as: (6).

$$L = T - V$$

$$\hat{Q}_k = \sum_{j=1} F_j \cdot \frac{\partial p_j}{\partial \hat{q}_k} = \frac{d}{dt} \frac{\partial L}{\partial \dot{\hat{q}}_k} - \frac{\partial L}{\partial \hat{q}_k} + \frac{\partial D}{\partial \dot{\hat{q}}_k} \quad (6)$$

where q_k is the k -th generalized coordinate and F_j corresponds to any forces acting on the system at point p_j . Assuming that no forces act on the system ($\hat{Q}_k = 0$) it is possible to write the pendulum's dynamics as the following second order system:

$$\mathbf{M} \ddot{\boldsymbol{\theta}} + \mathbf{C} \dot{\boldsymbol{\theta}} + \mathbf{G} = \boldsymbol{\tau} \quad (7)$$

where:

$$\boldsymbol{\theta} = [\theta_1 \ \theta_2]^T$$

$$\mathbf{M} = \begin{bmatrix} \alpha + 2\beta \cos \theta_2 & -(\gamma + \beta \cos \theta_2) \\ -(\gamma + \beta \cos \theta_2) & \gamma \end{bmatrix}$$

$$\mathbf{C} = \begin{bmatrix} -2\beta \dot{\theta}_2 \sin \theta_2 & \beta \dot{\theta}_2 \sin \theta_2 \\ \beta \dot{\theta}_1 \sin \theta_2 & 0 \end{bmatrix}$$

$$\mathbf{G} = \begin{bmatrix} \epsilon \sin \theta_{21} - \delta \sin \theta_1 \\ -\epsilon \sin \theta_{21} \end{bmatrix}$$

$$\boldsymbol{\tau} = - \begin{bmatrix} k_1 \theta_1 + b_1 \dot{\theta}_1 \\ k_2 \theta_2 + b_2 \dot{\theta}_2 \end{bmatrix}$$

$$\alpha = I_1 + I_2 + m_1 r_1^2 + m_2 (l_1^2 + r_2^2)$$

$$\beta = m_2 l_1 r_2$$

$$\gamma = I_2 + m_2 r_2^2$$

$$\delta = (m_1 r_1 + m_2 l_1) g$$

$$\epsilon = m_2 r_2 g$$

and g is the constant acceleration of gravity. We consider that the torque generated by the joint stiffness and damping parameters is such that the vertical orientation of the body segments corresponds to the equilibrium position.

Notice that the dynamics of the system presented in Fig. 1-b) is written only in terms of the measurable angular values θ_1 and θ_2 .

2.1 Parameter Estimation

It is possible to rewrite the second order model (7) as a linear function of the joint's visco-elastic parameters as follows:

$$\mathbf{Z} = \mathbf{H} \boldsymbol{\lambda} = -\boldsymbol{\tau} \quad (8)$$

$$\mathbf{H} = \begin{bmatrix} \theta_1 & \dot{\theta}_1 & 0 & 0 \\ 0 & 0 & \theta_2 & \dot{\theta}_2 \end{bmatrix} \quad (9)$$

where λ contains the desired stiffness and damping parameters:

$$\lambda = \begin{bmatrix} k_1 \\ b_1 \\ k_2 \\ b_2 \end{bmatrix} \quad (10)$$

Details regarding parameter estimation Consider the following linear system

$$\mathbf{Z} = \mathbf{H}\hat{\lambda} + \rho \quad (11)$$

where \mathbf{Z} is a measurement vector, $\hat{\lambda}$ are the system's estimated linear parameters, ρ an estimation error vector, and \mathbf{H} is known as the configuration matrix.

Least Squares Estimation Each row of \mathbf{Z} and \mathbf{H} represents one equation which can be used to solve the linear system defined by (8). Ideally, there should be *at least* enough linearly independent measurements such that \mathbf{H} is squared and invertible. In practice, measurements can be joined to create an overdetermined system (Khalil and Dombre, 2004). It is then possible to find a vector $\hat{\lambda} = \mathbf{H}^+\mathbf{Z}$ such that iEuclidean norm of ρ is minimized (Mooring et al., 1991). The Moore-Penrose pseudoinverse (Penrose, 1955) is generally used for this where $\mathbf{H}^+ = \left(\mathbf{H}^T\mathbf{H}\right)^{-1}\mathbf{H}^T$

Recursive Methods It is also possible to make use of a recursive method such as the Kalman filter to estimate a set of constant parameters (Simon, 2006). The Kalman filter equations are written as:

$$\hat{\lambda}_k^+ = \mathbf{A}\hat{\lambda}_k^- + \mathbf{B}\mu_k \quad (12)$$

$$\mathbf{P}_k^+ = \mathbf{A}\mathbf{P}_k^- \mathbf{A}^T + \mathbf{Q} \quad (13)$$

$$\mathbf{K}_k = \mathbf{P}_k^- \mathbf{H}^T \left(\mathbf{H}\mathbf{P}_k^- \mathbf{H}^T + \mathbf{R} \right)^{-1} \quad (14)$$

$$\hat{\lambda}_k = \hat{\lambda}_k^- + \mathbf{K}_k \left(\mathbf{Z}_k - \mathbf{H}\hat{\lambda}_k^- \right) \quad (15)$$

$$\mathbf{P}_k = (\mathbf{I} - \mathbf{K}_k\mathbf{H})\mathbf{P}_k^- \quad (16)$$

where \mathbf{A} and \mathbf{B} determine how the models parameters (λ) change over time; \mathbf{P} , \mathbf{Q} and \mathbf{R} are the estimation, process and measurement variance and covariance matrices respectively; \mathbf{Z} is the measurement vector; \mathbf{H} is the configuration matrix; \mathbf{K} is the Kalman gain; and \mathbf{I} is an identity matrix of suitable size.

2.2 Estimating the model parameters using simulated data

In order to create a set of data suitable for the parameter estimation outlined before, the second order model (7) was solved numerically using a fourth order Runge-Kutta approximation using a fixed step of 1 ms and the initial

conditions presented in Table 1. Thirty seconds of simulated data were obtained. The required biomechanical parameters (segment masses and lengths) were obtained from anthropometric tables (Winter, 2009) and correspond to a 1.7 m tall subject weighing 85 kg. They can be found in Table 2. The initial conditions given in Table 1 were chosen to comply with the *hold and release* method outlined by Bortolami et al. (2003), resulting in a life-like motion, and keeping the pendulum's overall center of mass within a distance from the ankle joint no larger than the subject estimated foot size.

Table 1. Initial conditions for numerical simulation.

| Initial condition | | | | | |
|-------------------|-------|-------|------------------|---|-------|
| θ_1 | -0.17 | rad | θ_2 | 0 | rad |
| $\dot{\theta}_1$ | 0 | rad/s | $\dot{\theta}_2$ | 0 | rad/s |

Table 2. Parameters used for the simulation of the second order model of human balance.

| Param. | Value | Param. | Value |
|--------|-----------|--------|-------------|
| M | 85 kg | k_1 | 1050 Nm/rad |
| h | 1.7 m | b_1 | 30 Nms/rad |
| m_1 | 0.322M kg | k_2 | 500 Nm/rad |
| m_2 | 0.678M kg | b_2 | 10 Nms/rad |
| l_1 | 0.53h m | | |
| r_1 | 0.29h m | | |
| r_2 | 0.18h m | | |

The model's parameters were estimated using the least squares and recursive approaches introduced in the previous section. The estimated visco-elastic parameter values ($\hat{\lambda}_{ideal}$) were obtained after substituting the values of θ from simulation and $\dot{\theta}$, and $\ddot{\theta}$ calculated numerically in \mathbf{Z} and \mathbf{H} . In an attempt to reduce estimation errors due to phase shift, the central differences method was used for calculating the time derivatives (Khalil and Dombre, 2004).

To accurately replicate a real-world experiment, normally distributed noise was added to the orientation of each segment obtained from simulation. Prior to calculating the derivatives, it was then necessary to remove some high frequency noise introduced. This was done using a zero-phase, low-pass Butterworth filter with a cut-off frequency of 25 Hz (Khalil and Dombre, 2004) and is required as angular velocity and acceleration can only be obtained through numerical methods.

The filtered values for angular position, velocity and acceleration are used to estimate the value of the model's visco-elastic parameter using a least squares approach ($\hat{\lambda}_{LSM}$) by substituting them in \mathbf{Z} and \mathbf{H} . They were also used to estimate the parameters' value ($\hat{\lambda}_{KF}$) by means of a Kalman filter.

To evaluate the accuracy of the parameter estimation we define the error as $e_i = \mathbf{Z} - \mathbf{H}_i\hat{\lambda}_i$. This error will be null when $\hat{\lambda} = \lambda$. For the sake of readability we report only its average and standard deviation



Fig. 2. Prototype built to validate the parameter estimation procedure. The stiffness at the joints was simulated using linear springs between the joints. To reduce friction, all contact surfaces were covered with teflon.

3. PARAMETER ESTIMATION USING EXPERIMENTAL DATA

A double inverted pendulum prototype was built (see Figure 2) to test the parameter estimation protocol described in the previous section. Linear springs were used to stiffen the prototype's joints. The size and mass of its segments was measured and are presented in Table 3. For the configuration shown in Figure 2, and for small angular displacements it is expected that the rotational stiffness $k_r = k_l r^2$; where k_r is the rotational stiffness k_l is the linear stiffness of the spring and r the corresponding moment arm. Four linear springs with a constant of 850 N/m were used on the model's first joint (simulating the ankle) and were placed to have a moment arm of 74.2 mm around it. In the same way two springs with a constant of 690 N/m were used on the second joint (hip) and placed to have a moment arm of 37.1 mm. Additionally the resting lengths of the springs are such that while the prototype is in motion two of the spring at the ankle joint may become relaxed while the ones at the hip joint remain taut. That is, the approximated stiffness of the joints is expected to be of 9.38 Nm/rad and 1.88 Nm/rad for the prototype's ankle and hip joints respectively. To reduce friction all contact surfaces were covered with teflon. Other than friction and air resistance, no damping elements were considered.

Table 3. Measured model parameters for a double inverted pendulum.

| Param. | Value | Param. | Value |
|--------|---------|--------|-----------------|
| m_1 | 0.25 kg | k_1 | 9.38 Nm/rad |
| m_2 | 0.20 kg | b_1 | unknown Nms/rad |
| l_1 | 0.53 m | k_2 | 1.88 Nm/rad |
| r_1 | 0.27 m | b_2 | unknown Nms/rad |
| r_2 | 0.23 m | | |

During the experiment the pendulum was moved to a random initial position, held there at rest, and then suddenly

released. The orientation of each segment was measured by tracking three passive markers (corresponding to the ankle, hip, and head of the prototype) using the open sourced software Kinovea. The sampling frequency was that of the RGB-cameras used and averaged 22.5 fps. In order to obtain an overdetermined system for the parameters estimation the experiment was repeated eight times and the respective measurements aggregated.

Data from one additional was obtained for validation. This was done by predicting the angular displacement of the prototype by means of a numerical simulation, and comparing it to the measured data.

4. DISCUSSION AND RESULTS

Table 4. Estimated values and estimation error for the second order model's visco-elastic parameters.

| Param. | $\hat{\lambda}_{ideal}$ | $\hat{\lambda}_{LSM}$ | $\hat{\lambda}_{KF}$ | |
|---------------------|-------------------------|-----------------------|----------------------|---------|
| \hat{k}_1 | 1050.0 | 1084.1 | 931.5 | Nm/rad |
| \hat{b}_1 | 30.0 | 28.6 | 39.9 | Nms/rad |
| \hat{k}_2 | 500.0 | 506.0 | 388.1 | Nm/rad |
| \hat{b}_2 | 10.0 | 8.3 | 6.7 | Nms/rad |
| $\text{mean}(\rho)$ | $-0.72E-6$ | $-1.53E-2$ | $-0.17E-2$ | Nm |
| $\text{std}(\rho)$ | $8.9E-9$ | 0.21 | 0.21 | Nm |

Table 5. Prototype's estimated visco-elastic parameter.

| Param. | $\hat{\lambda}$ |
|-------------|-----------------|
| \hat{k}_1 | 9.84 Nm/rad |
| \hat{b}_1 | 0.16 Nms/rad |
| \hat{k}_2 | 1.86 Nm/rad |
| \hat{b}_2 | 0.02 Nms/rad |

Angular trajectories obtained through the numerical solution of (7) are shown in Fig. 3. The blue line represents the noisy angular values while the red dashed line shows the values after filtering using a zero-phase Butterworth filter. A good match, with no visible phase shift, between both curves is observed.

Using the data obtained from simulation Table 4 shows the values obtained for the model's visco-elastic parameter estimated from noiseless data and from filtered data using the least squares and the Kalman filter approaches. Figure 4 shows the evolution of the parameter estimate using the recursive approach. Table 4 also shows the average and standard deviation error obtained with each parameter vector. Notice that while the parameters estimated with each method vary, the estimation error is small for all three vectors. That is, while $\hat{\lambda}_{ideal}$ estimated the parameter values exactly, both $\hat{\lambda}_{LSM}$ and $\hat{\lambda}_{KF}$ contain suitable values for modeling the simulated data.

These results assume constant visco-elastic parameters. However, muscle contraction will change the apparent stiffness of the joint (Roberts and Azizi, 2011) possibly making the least squares approach unsuitable. This is not

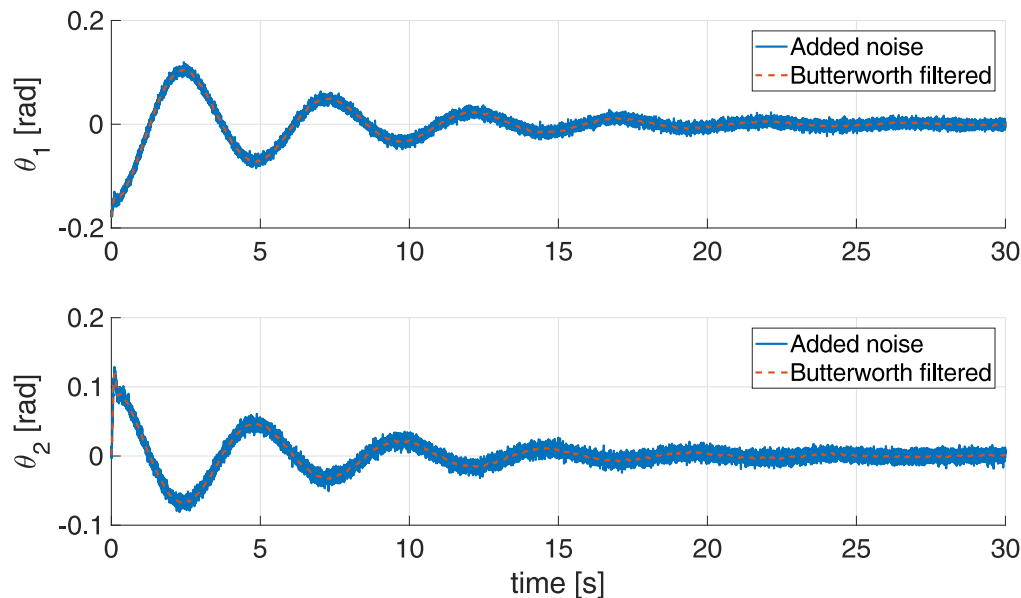


Fig. 3. Simulated angular value for the orientation of each of the model's segment. The blue line represents the noisy angular values while the red dashed line shows the values after the application of the zero-phase Butterworth filter.

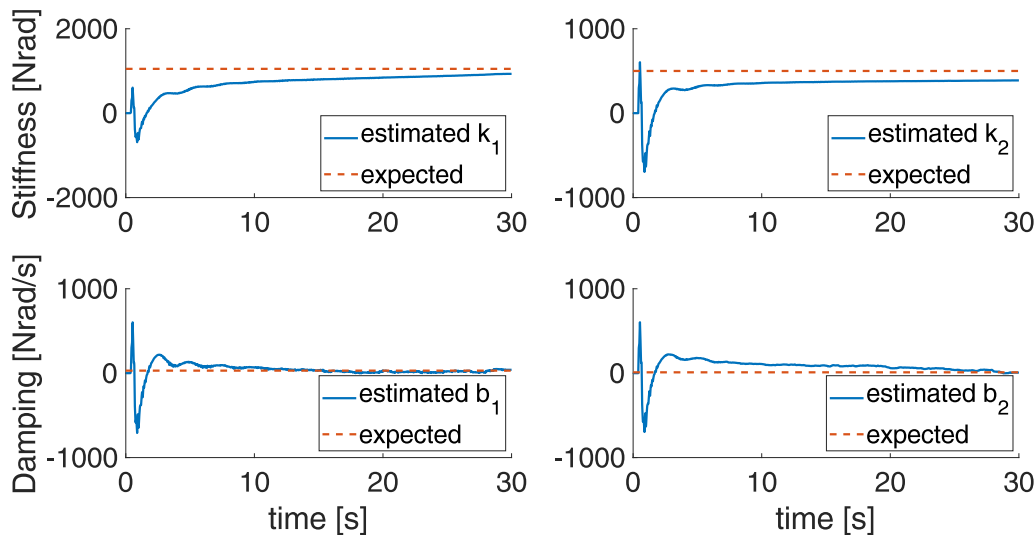


Fig. 4. Estimated values for the model's visco-elastic parameter using a recursive method from low-pass filtered noisy data. The blue line shows the evolution of the parameter value as more information is available. The red dashed line shows the value used for simulation.

as limitation of the dynamic model (7) and may favor the implementation of the Kalman Filter as it can be used to estimate time-changing parameters.

Regarding the prototype, its estimated values are given in Table 5. Figure 5 shows: in blue the measured angular trajectory obtained with the prototype for a validation trial not used for the parameter estimation, while the red dashed line is the prototype's predicted trajectory using

the estimated parameter values. Overall there is a good match with respect to peak height, but the measured data seems to have a higher natural frequency. This is partially explained as the estimated parameters assume a linear behavior of the equivalent rotation spring which may not be the case due to large angles between its segments. It is may also be the case that an improper sampling frequency from the RGB-camera contributed to the estimation error of the prototype's damping. Note from Figures 3 and 5

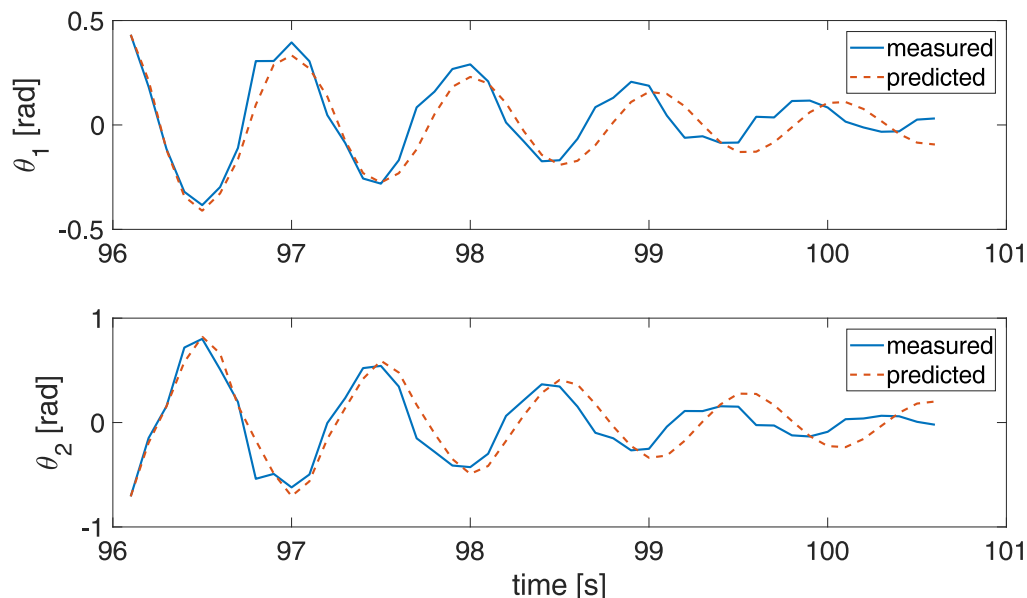


Fig. 5. Angular trajectory validation for the prototype using the estimated values for the visco-elastic parameters. The blue line is the measured trajectory on a validation trial (not used for parameter estimation) while the red dashed line is the prototype's predicted trajectory.

that the prototype exhibits a higher resonant frequency than the simulated human by almost a factor of five and thus a higher sampling frequency is desired.

5. CONCLUSION

The results presented here show the feasibility of estimating stiffness and damping parameters in human joints while balancing. Future work should focus on using experimental data gathered from human subjects. It should also focus on the estimation of visco-elastic parameters of both tendons and muscles in the ankle and hip joints by extending the third order model proposed by Coronado et al. (2015) by allowing for a hip joint.

REFERENCES

- Bortolami, S.B., DiZio, P., Rabin, E., and Lackner, J. (2003). Analysis of human postural responses to recoverable falls. *Experimental brain research*, 151(3), 387–404.
- Chavez-Romero, R., Cardenas, A., and Piovesan, D. (2014). Viscoelastic properties of the ankle during quiet standing via raster images and ekf. In *2014 IEEE Signal Processing in Medicine and Biology Symposium, IEEE SPMB 2014 - Proceedings*.
- Coronado, L.E., Chavez-Romero, R., Maya, M., Cardenas, A., and Piovesan, D. (2015). Combining genetic algorithms and extended kalman filter to estimate ankle's muscle-tendon parameters. In *ASME 2015 Dynamic Systems and Control Conference*, V001T15A002–V001T15A002. American Society of Mechanical Engineers.
- Khalil, W. and Dombre, E. (2004). *Modeling, Identification & Control of Robots*. Kogan Page Science, London, UK.
- Meirovitch, L. (2010). *Methods of analytical dynamics*. Courier Corporation.
- Menz, H.B., Morris, M.E., and Lord, S.R. (2005). Foot and ankle characteristics associated with impaired balance and functional ability in older people. *The Journals of Gerontology: Series A*, 60(12), 1546–1552.
- Mooring, B.W., Roth, Z.S., and Driels, M.R. (1991). *Fundamentals of Manipulator Calibration*. John Wiley & Sons, Inc, New York, USA.
- Ogata, K. (1998). *System dynamics*, volume 3. Prentice Hall New Jersey.
- Penrose, R. (1955). A generalized inverse for matrices. *Mathematical proceedings of the Cambridge Philosophical Society*, 51, 406–413.
- Piovesan, D., Kennett, C., Chavez-Romero, R., Panza, M.J., and Cárdenas, A. (2015). Stiffness boundary conditions for critical damping in balance recovery. In *ASME 2015 International Mechanical Engineering Congress and Exposition*, V003T03A066–V003T03A066. American Society of Mechanical Engineers.
- Roberts, T.J. and Azizi, E. (2011). Flexible mechanisms: the diverse roles of biological springs in vertebrate movement. *Journal of Experimental Biology*, 214(3), 353–361.
- Simon, D. (2006). *Optimal state estimation: Kalman, H infinity, and nonlinear approaches*. John Wiley & Sons.
- Winter, D.A. (2009). *Biomechanics and motor control of human movement*. John Wiley & Sons.